5-2013

Synthesis of Isotopologues and Nanoparticles for Hyper Raman Spectroscopy

Burton K. Mandrell
University of Tennessee Knoxville, bmandre1@utk.edu

Synthesis of Isotopologues and Nanoparticles for Hyper Raman Spectroscopy

Burton K. Mandrell

Department of Chemistry

Chancellor's Honors Program

University of Tennessee, Knoxville

Thesis Committee:

Dr. Jon Camden

Dr. Michael Best

Dr. Jeffrey Kovac

Senior Honor's Thesis

May 2013

Table of Contents:

Abstract:

In order to conduct single molecule hyper Raman spectroscopy, new isotopologues (molecules that differ only by isotopic composition) of rhodamine 6G (R6G) and crystal violet (CV) are proposed and synthesized. Previous isotopologues of R6G are shown to be indistinguishable in hyper Raman which prevents confirmation of single molecule spectroscopy. A new isotopologue of R6G is proposed where the deuteriums are added into the xanthene ring in order to distinguish the hyper Raman active vibrational modes as compared to R6G-d0. The key to deuterating the xanthene ring is to deuterate the 3-(ethylamino)-p-cresol starting material through electrophilic aromatic substitution of sulfuric acid-d2 while protecting the aryl amine to ensure the ring remains activated. However, this synthesis of R6G-d2 was not completed. The synthetic target was then shifted to the more synthetically accessible CV-d30 which was successfully synthesized and characterized for the first time. Initial hyper Raman studies of CV-d30 shows that CV-d30 is distinguishable from CV-d0 in hyper Raman which makes these isotopologues viable candidates for single molecule hyper Raman studies. Previous work on the shape-controlled syntheses of plasmonic nanoparticles is also presented. The synthesis of nanoparticles provided initial, fundamental experience for the lab in synthesis for the purpose of imaging and studying plasmonics.

1. Introduction

1.1 Molecular Vibrations[1]

The vibrations of a diatomic molecule can be modeled classically by Hooke's Law and Newton's 2nd Law of Motion:

$$\mu\frac{d^2x}{dt^2} + kx = 0 \qquad \text{(Eq. 1.1a)}$$

Where x is the displacement from equilibrium bond length, k is the spring constant, and μ is the reduced mass of the molecule. Eq. 1.1a is a linear ordinary differential equation whose general solution is:

$$x(t) = Asin(\omega t + \varphi) \qquad \text{(Eq. 1.1b)}$$

Where A is the amplitude of the vibration, t is time, φ is the phase angle, and ω is the frequency of the vibration which can be further reduced as:

$$\omega = \sqrt{\frac{k}{\mu}} \qquad \text{(Eq. 1.1c)}$$

Eq. 1.1b is critically important because it relates the reduced mass of the system to the frequency of the vibration. The energy of the vibrations can be modeled quantum mechanically using the one-dimension Schrodinger equation:

$$-\frac{\hbar^2}{2\mu}\frac{d^2\psi}{dx^2} + V(x)\psi(x) = E\psi(x) \qquad \text{(Eq. 1.1d)}$$

Inputting the potential energy function $V(x) = \frac{1}{2}kx^2$ for a spring into Eq. 1.1c:

$$-\frac{\hbar^2}{2\mu}\frac{d^2\psi}{dx^2} + \frac{1}{2}kx^2\psi(x) = E\psi(x) \qquad \text{(Eq. 1.1e)}$$

Which can be solved as an eigenvalue/eigenvector problem to give quantized solutions:

$$E_n = \hbar\omega(n + \tfrac{1}{2}) \qquad \text{(Eq. 1.1f)}$$

where n = 0,1,2,3… which corresponds to a particular vibrational state of the molecule. Inputting Eq. 1.1b into Eq. 1.1d shows the mass dependence on the energy of a vibration:

$$E_n = \hbar\sqrt{\frac{k}{\mu}}(n + \tfrac{1}{2}) \qquad \text{(Eq. 1.1g)}$$

The mass dependence is *inversely proportional* to the energy of the vibration such that an increase in the reduced mass decreases the vibrational energy. Although anharmonicities

corrections can be added to increase the accuracy of the model, the mass dependence does not change. This means that molecular vibrations are sensitive to changes in the reduced mass such that vibrational spectroscopy can resolve isotopic substitutions in a molecule. For example, Figure 1 shows the ro-vibrational spectrum of HCl where the taller peaks corresponds to $H^{35}Cl$ and the smaller peaks that are red shifted are the heavier $H^{37}Cl$ peaks which agree with the natural abundance of ^{35}Cl:^{37}Cl of 2:1.

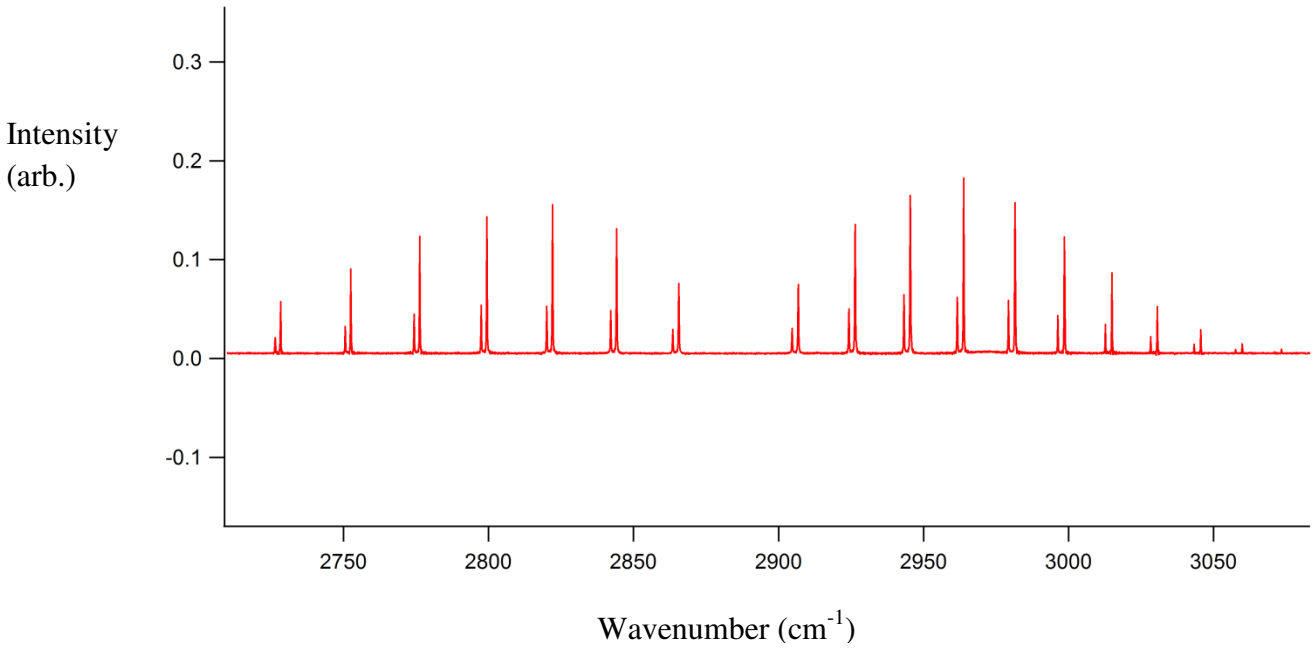

Figure 1: Ro-vibrational spectrum of gas phase HCl taken.

1.2 Raman Spectroscopy

Raman scattering was discovered in 1928 and led to a Nobel Prize in 1930 to C.V. Raman, an Indian physicist.[2] Raman scattering is the inelastic scattering of light. In a typical experiment, monochromatic light of frequency ω irradiates a molecule of interest which scatters light. The scattered light consists of Rayleigh scattered light of frequency ω and Raman scattered light of frequency $\omega \pm \omega_v$ where ω_v corresponds to the energy of a vibrational transition. Raman scattering is a result of the light-driven electric dipoles with frequency dependent oscillations:

$$\mu_0(\omega \pm \omega_v) = \alpha^{Ram} \cdot E_0(\omega) \qquad \text{(Eq. 1.2a)}$$

Where μ_0 is the time-independent amplitudes of the induced electric dipoles at frequency ω, $E_0(\omega)$ is the time-independent amplitude of the incident electric field of frequency ω, and α^{Ram} is the polarizability associated with the molecular states probed by the incident field.[3] More

simply, the dipole moment of a molecule is proportional to the product of the polarizability of the molecule times the magnitude of the incident electric field.

Raman spectroscopy is a versatile vibrational technique. Raman scattering can occur in the visible wavelength where detection methods are more sensitive, and more light sources are available whereas infrared (IR) spectroscopy uses infrared light which requires different light sources and detectors. The biggest advantage of Raman scattering over IR is that Raman spectroscopy can measure analytes in solution which bypasses complicated sample preparation required for IR. This is possible because the Raman cross section of water is very small, and organic solvent's vibrational modes can be subtracted as background. Raman is advantageous over fluorescence spectroscopy as well. Fluorescence spectroscopy/microscopy requires that the analyte be fluorescent. Adding fluorescent tags to an analyte to allow fluorescence spectroscopy can change the chemical and physical properties of the analyte. Raman spectroscopy can be applied to non-fluorescent molecules as well as fluorescent molecules. Raman spectroscopy can be conducted off resonance of the electronic states while fluorescence can only be measured at specific wavelengths at which the molecule will absorb and fluoresce.

The main disadvantage of Raman is that it is a weak process. Only 1 out of 10^6 scattered photons are Raman scattered. The vast majority of the photons are elastically scattered as Rayleigh light. However, Raman signal can be drastically enhanced by using resonance Raman scattering or plasmonics. Resonance Raman scattering is where the incident light overlaps (resonant) or is in proximity (pre-resonant) to a real electronic state of the molecule. This can add $10^{2\text{-}6}$ orders of magnitude to Raman signal by increasing the probability of scattering events. Plasmons are the conductive oscillation of electrons on a metal. Silver and gold nanoparticles are well known to support a localized surface plasmon resonance that can enhance local electric fields. Putting a molecule in a plasmon can increase Raman scattering by $10^{6\text{-}8}$ by increasing the local electric field. This increase in the applied electric field increases the magnitude of the light-induced dipoles (Eq. 1.2a).

1.3 Hyper Raman

Hyper Raman is the two photon analog of Raman. If the incident light has frequency ω, the hyper Raman scattering occurs at $2\omega \pm \omega_v$. Hyper Raman is compared to Raman in Figure 2. The most interesting aspect of hyper Raman is that hyper Raman can probe vibrations that are 1 photon forbidden because hyper Raman is a 2 photon process.[4] This can further lead to insight into the symmetry of electronic states. The disadvantage of hyper Raman is that it is an extremely weak process – 10^6 times weaker than Raman. However, resonance effects and plasmonics can enhance hyper Raman to make hyper Raman comparable in signal to Raman.

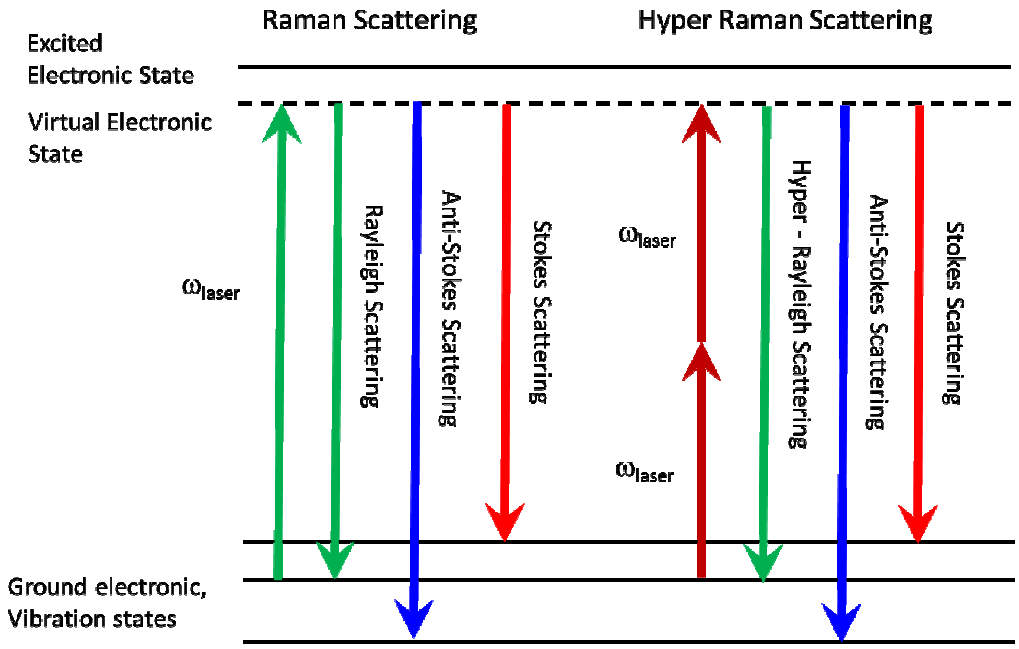

Figure 2: Jablonski diagram of Raman scattering (left) and Hyper Raman scattering (right).

1.4 Single Molecule Spectroscopy

Single molecule spectroscopy is taking measurements of single molecules instead of the ensemble bulk average. Because measurements are limited by signal to noise ratios, optical measurements are usually conducted using probe volumes that contain orders of magnitude of molecules. The tradeoff of gaining large signal from multiple molecules is the loss of information about specific molecular environments and the *distribution* of the measured values.[5] Confirmation that a spectrum can be attributed to one molecule requires statistical evidence. Fluorescence measurements paved the way for single molecule spectroscopy since the early 1990's with confirmations stemming from limiting the probe volume of a laser while reducing the number of excitable molecules within the probe volume.[6] In surface enhanced Raman, molecules are adsorbed on a plasmonic nanostructure in such a way that the number of adsorbed molecules can not be exactly known due to a strong distance dependence of the electric field enhancement caused by the plasmon.[7] This makes signal intensity analysis through the lens of statistics invalid for quantizing the number of molecules in the probe volume.[8] Etchegoin et. al. provided a different approach to prove single molecule Raman through a bi-analyte method where two different molecules are measured in time where the differences in the vibrational signatures of both molecules can be used to determine if one type of molecule is observed.[9]

Although this technique uses the vibrational information to determine single molecules, differences in surface adsorption chemistries and Raman cross-sections obscure the number of events occurring. Also, different molecules will likely have different electronic absorptions meaning both molecules will likely not be excited on resonance at the same time. The bi-analyte technique was improved through the use of isotopologues- two molecules that differ only by isotopic composition. Isotopologues are advantageous because they have the same Raman cross section, the same electronic states, and the same surface chemistries.[10] Using a 50:50 mixture of isotopologues, the silver nanoparticles are vibrationally probed and sampled. If multiple molecules are sampled, the probability of observed spectra follow the binomial distribution where the probability of seeing only 1 isotopologue in a spectrum is equal to $\frac{1}{2^n}$ where n is the number of molecules per sample. For example, if a nanoparticle is probed, and there are 2 molecules in the probe volume, then the probability that both are isotopologue A is 25%, both isotopologue B is 25%, and mixed AB is 50%. If 100 nanoparticles are sampled, each with 2 molecules, then the total frequency of events would look like Figure 3a. If only 1 molecule is found per nanoparticle, the frequency distribution would look like Figure 3b.

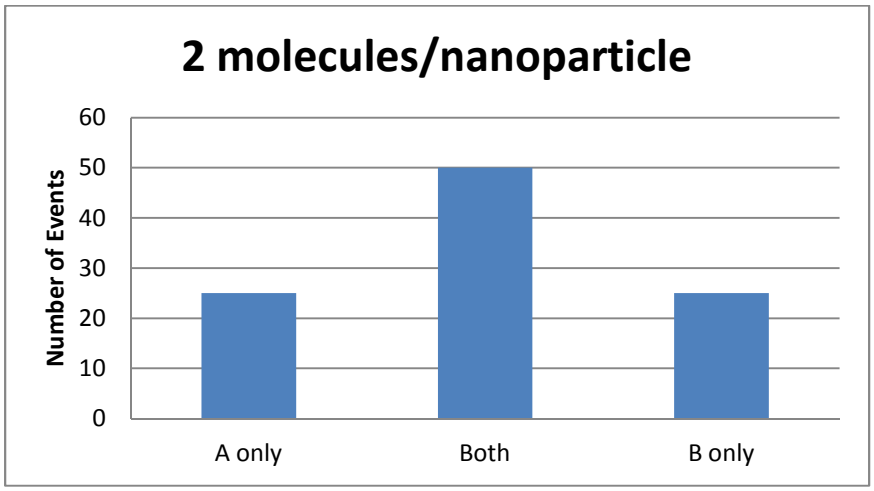

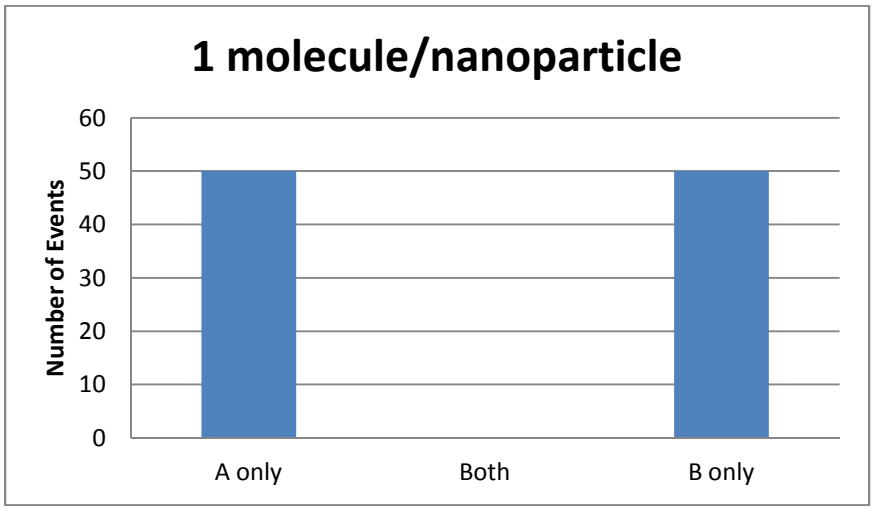

Figure 3a (top): Frequency distribution showing 1:2:1 ratio of spectra with A only, Both, or B only resulting from 2 molecules in probe volume.

Figure 3b (bottom): Frequency distribution showing 1:0:1 ratio of spectra with A only, Both, or B only resulting from 1 molecule in probe volume.

By controlling the relative concentration of analyte to nanoparticles, these distributions can be controlled so that on average only 1 molecule per nanoparticle is seen. Measuring the frequency distribution is a statistically sound proof to confirm single molecule spectroscopy. The key to this proof is that the isotopologues must be vibrationally distinguishable so that one can assign a specific vibrational spectrum as being A only, B only, or having vibrational signatures of both molecules. Having isotopologues that are vibrationally distinguishable in hyper Raman has been the primary problem with single molecule hyper Raman thus far. We have found that the surface enhanced hyper Raman spectrum of R6G-d4 is identical to R6G-d4 (Figure 4) which is the primary motivation to synthesize other isotopologues.

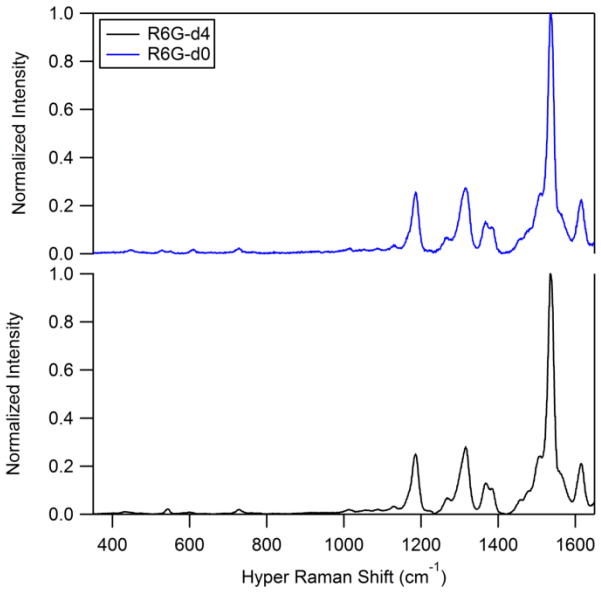

Figure 4: Surface enhanced hyper Raman (SEHRS) of R6G-d0 (blue) and R6G-d4 (black) on silver colloids at 1064 nm. The two isotopologues are indistinguishable which disallows SM-SEHRS.

2. Synthesis of Plasmonic Nanoparticles

The plasmon of a metallic nanoparticle is a function of the size, shape, and local environment of a nanoparticle.[11] In order to tune the plasmonic properties of a nanoparticle, the size and shape of the particle must be synthetically tailored. Over the last 10-15 years, the shape-controlled synthesis of nanoparticles of vastly different geometric shapes, compositions, and sizes have been published. These syntheses provide the needed substrates to study the fundamental questions of plasmonics. Herein, the syntheses of various published techniques were attempted to be reproduced.

The most widely used nanoparticle synthesis for surface enhanced Raman is the Lee and Meisel synthesis where silver nitrate is reduced by sodium citrate in boiling water.[12] The resulting silver nanoparticles are widely dispersed in size and shape which is manifested in broad uv-vis extinction. [uv-vis] However, theoretical calculations of the electromagnetic field enhancement from a surface plasmon suggests that nanoparticles with sharp corners and their dimers have the highest enhancement intensities (Figure 5).[13] Synthesizing solutions that contained primarily sharp cornered nanoparticles could provide a better substrate for spectroscopy as compared to the random assortment provided by the Lee and Meisel synthesis.

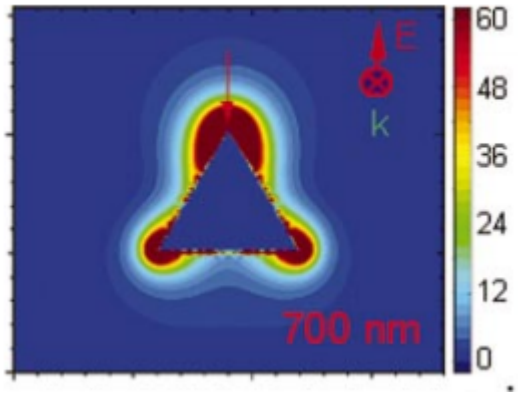

Figure 5: Electromagnetic enhancement of a silver triangular nanoprism excited by 700 nm light.[13]

The key to modern syntheses of silver and gold nanoparticles rely on controlling the kinetics of metal ion reduction while selectively depositing the metal on specific crystal faces to direct the formation of specific shapes.[14] This is done by varying the temperature, reducing agent, and the "capping agent"- a molecule that selectively binds to faces of the developing crystal to direct the formation of particular shapes. The attempted synthesized shapes have been silver cubes[15], silver bipyramids[16], and gold spheres[17] with most of the synthetic effort being devoted to light-driven conversion of silver spheres to silver triangles.[18]

The silver cubes were synthesized in ethylene glycol at 140°C in the presence of hydrochloric acid and poly(vinyl pyrrolidone) with average molecular weight ~55,000. Ethylene glycol serves as both the solvent and the reducing agent in this synthesis; upon heating, ethylene glycol oxidizes to acetaldehyde which is a mild reducing agent. The kinetics of acetaldehyde formation governs the rate of the silver reduction.[15] Using a similar technique, silver bipyramids are synthesized by adding sodium bromide instead of using hydrochloric acid.[16] These syntheses were not successfully reproduced, mainly because of irregular temperature control. The syntheses were conducted in a custom built oil bath where silicone oil was contained in an aluminum dish. An aluminum stage was built to hold a glass vial while stirring the oil with a paper clip (Figure 6). Temperature was measured using a 200°C mercury thermometer. A better method to conduct high temperature syntheses would be to use a hot plate with better temperature control that has a temperature probe.

2.1 Silver cube synthesis[15]: In a 20 mL glass disposable vial, 5 mL of anhydrous ethylene glycol is capped and heated at 140°C for 1 hour. 1 mL of 3mM HCl in ethylene glycol is quickly added and recapped. The solution then sits for 10 minutes after which 3 mL of 94 mM $AgNO_3$ in ethylene glycol and 3 mL of 147 mM poly(vinyl prryolidone) in ethylene glycol are added simultaneously with a Pasteur pipette at approximately 0.75 mL/minute. Afterwards, the solution is capped and heated for 5 minutes.

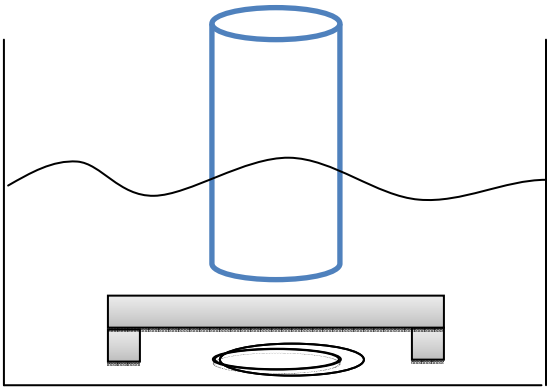

Figure 6: Custom built aluminum stage with paper clip to stir and silicone oil for heating.

Gold spheres were synthesized using the analogous synthetic method of the silver colloids where sodium citrate is boiled in the presence of chloroauric acid $HAuCl_4$.[17] Unlike the Lee and Miesel synthesis, the gold colloids made this way are predominately spheres. Upon reduction, the colloids turned a dark red color whose uv-vis is shown in Figure 7. The shapes are confirmed by transmission electron microscopy (TEM) as seen in Figure 8.

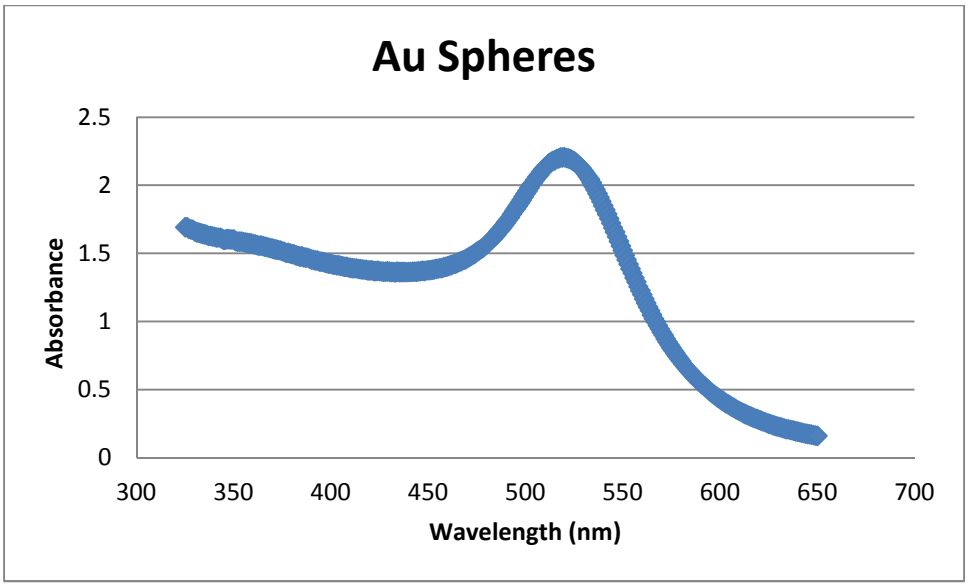

Figure 7: UV-Vis extinction of Au spheres in water.

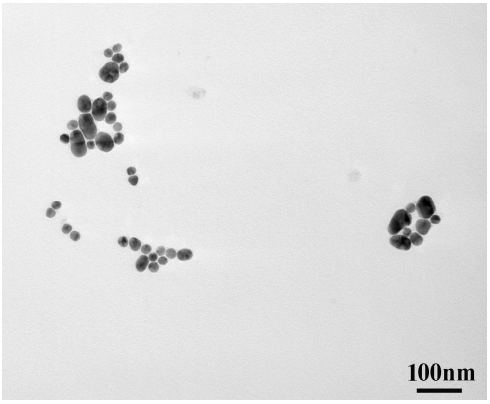

Figure 8: TEM image of Au spheres.

2.2 Gold sphere synthesis[17]: In a 250 mL Erlenmeyer flask cleaned by aqua regia (3:1 HCl:HNO_3), 50 mL of 1 mM $HAuCl_4$ was brought to a boil with vigorous magnetic stirring. Then, 5 mL of 38.8 mM sodium citrate was rapidly added. The solution was boiled for 10 minutes. Afterwards, the heat was turned off, and the solution was stirred for 15 more minutes. The resulting colloids were stored in 20 mL disposable glass vials.

Silver triangles are synthesized from a seed mediated approach where silver spheres of 5-10 nm are irradiated by light which photochemically oxidizes citrate while reducing silver nitrate. This synthesis is a two-step process where the very small silver seeds are synthesized first and then irradiated to form silver triangles. Although multiple papers have been published studying the mechanism of the synthesis including concentration studies and capping agents[19], the synthesis is still notoriously hard to reproduce with conflicting claims in the literature. Because the silver seeds must be very small to serve as substrates for triangle formation, a different synthetic approach is needed. Silver seeds are synthesized using a strong reducing agent, sodium borohydride. In the initial publication, the silver seeds were formed at room temperature with suggestion that a capping agent, bis(*p*-sulfonatophenyl) phenylphosphine dihydrate dipotassium salt (BSPP).[18] This seed solution was also irradiated with a conventional, broadband fluorescent lamp. Later publications definitively say that BSPP is not needed,[20] but then show mechanistic studies saying BSPP is necessary.[19] This led to a broad range of experiments testing the need of BSPP, the temperature of the synthesis, and the light source for the formation of triangles.

The first attempts at triangle synthesis did not use BSPP and were conducted at room temperature. In a typical synthesis, 95 mL milliQ water, 2 mL 5mM $AgNO_3$, 1 mL 30 mM sodium citrate, and 50 mM $NaBH_4$ were mixed in a 250 mL round bottom flask cleaned with aqua regia. The solution was stirred with a magnetic stir bar for 15 minutes after $NaBH_4$ addition. For the first several attempts, the colloids would crash out and form a black precipitant. The addition of the BSPP helped stabilize the colloids and prevented crashing out. The early attempts also used a standard fluorescent lamp found in a study desk, where samples were taped directly onto the light and left overnight. Later, a broad band, 100 W light source was acquired and a 510 ± 10 nm bandpass filter was used to direct specific size triangles.[20] Although monodisperse silver triangles in high yield were never attained, much work was done to navigate through the complicated literature and develop nanoparticle synthetic experience for the lab.

2.3 Silver triangle synthesis[19]: In a 250 mL round bottom flask cleaned with aqua regia and thoroughly rinsed (5 times) with milliQ water, 95 mL of milliQ water, 0.5 mL 20 mM silver nitrate, and 1 mL 30 mM trisodium citrate were stirred vigorously in an ice bath for 30 minutes while under nitrogen. Afterwards, freshly prepared 1mL 50 mM $NaBH_4$ is rapidly injected into the stirring solution. Then 5 drops of the 50 mM $NaBH_4$ solution are added every 2 minutes for 14 minutes. Afterwards, 1 mL of the 50 mM $NaBH_4$ solution is added dropwise simultaneously with 1 mL 5 mM BSPP solution added very slowly, dropwise. The resulting solution is then stirred in air while maintaining the ice bath over the course of 3 hours. Afterwards, the seed solution is pipetted 20 mL into 25 mL glass vials and refrigerated overnight. The following day, 350 µL of 0.1 M NaOH is added to the seeds and then irradiated using ~80% maximum intensity of the lamp with the bandpass filter. The seeds are irradiated for 5-30 hours.

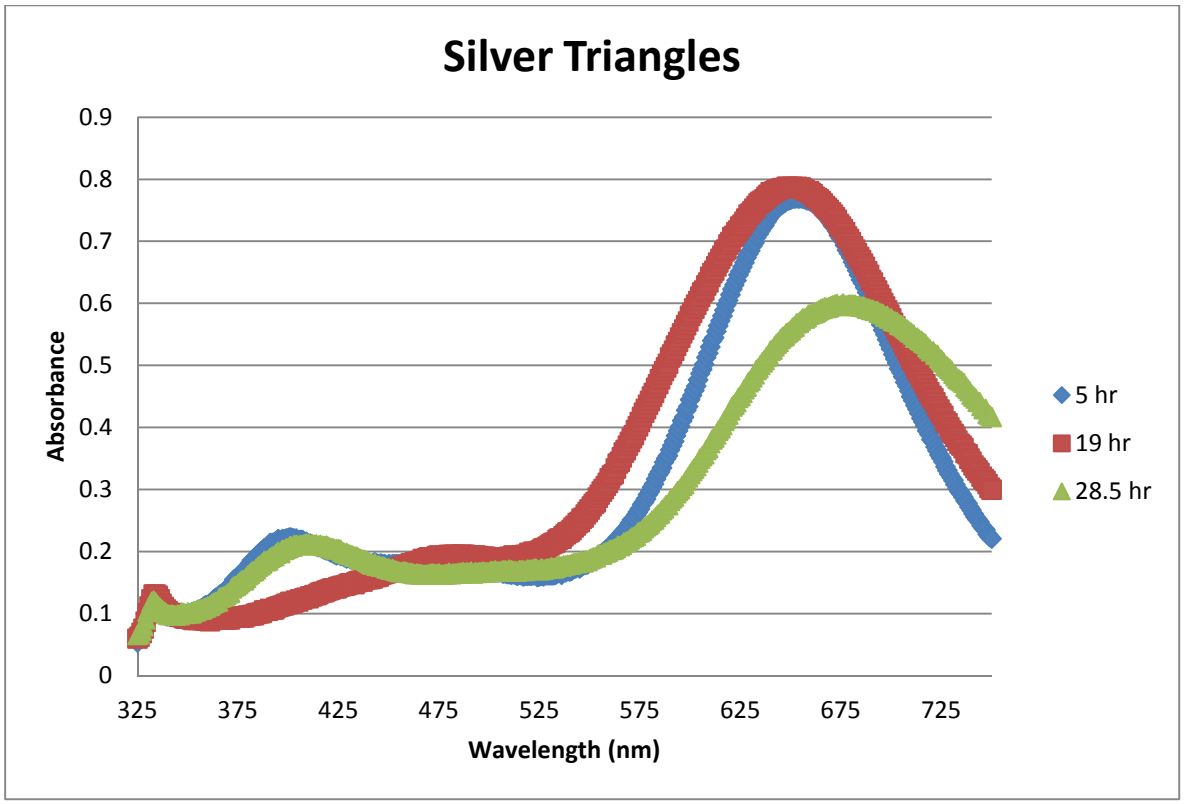

Figure 9: UV-Vis extinction of silver triangles with λ_{max} = 650 nm which is indicative of triangles.

3. Synthesis of Rhodamine 6G

Rhodamine 6G (R6G) is a molecule with one of the highest Raman scattering cross-sections and was one of the first molecules to observe single molecule surface enhanced Raman scattering (SM-SERS). R6G was also the first molecule to have been synthesized for isotopologue studies of SERS. R6G is a good synthetic target for Raman studies. The R6G isotopologue used for SM-SERS was the R6G-d4 which is shown in Figure 10. The synthetic scheme is shown in Figure 11.

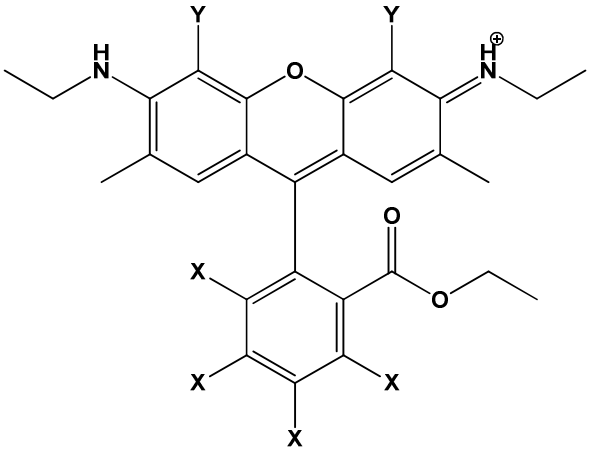

Figure 10: Isotopologues of Rhodamine 6G.
R6G-d0: X,Y =H
R6G-d2: Y = D
R6G-d4: X = D

The key to the R6G-d4 synthesis is the commercial availability of pthalic anhydride-d4. As stated, R6G-d4 has been synthesized previously and resulted in a spectral shift in the SERS spectra between R6G-d4 and R6G-d0. R6G-d4 thus served as the starting point for hyper Raman studies. However, it was soon discovered that R6G-d0 and R6G-d4 are indistinguishable in hyper Raman (Figure 4) which means that the isotopologues could not be used for single molecule hyper Raman. A new synthetic target was needed. Theoretical calculations of hyper Raman spectra conducted by Dr. Lasse Jensen at Penn State University suggested that the hyper Raman modes of R6G are localized in the xanthene ring. A synthetic scheme was then designed by Dr. Michael Best and Heidi Bostic to deuterate the xanthene ring of R6G (Figure 12).

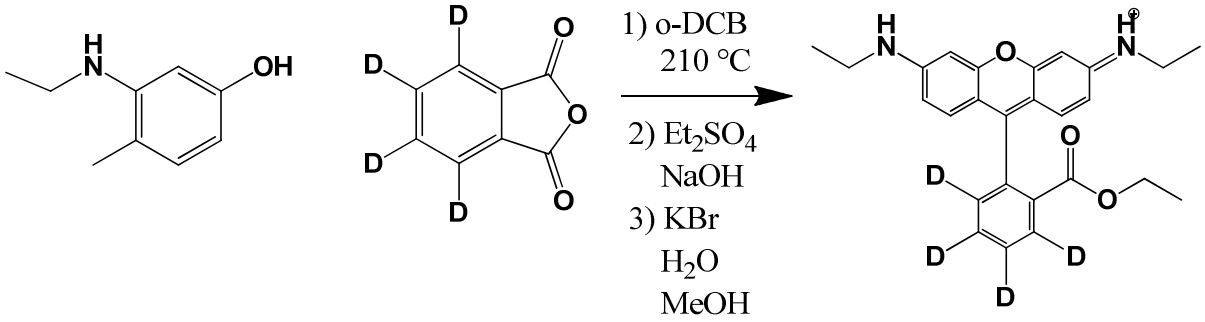

Figure 11: Synthetic Scheme of R6G-d4.

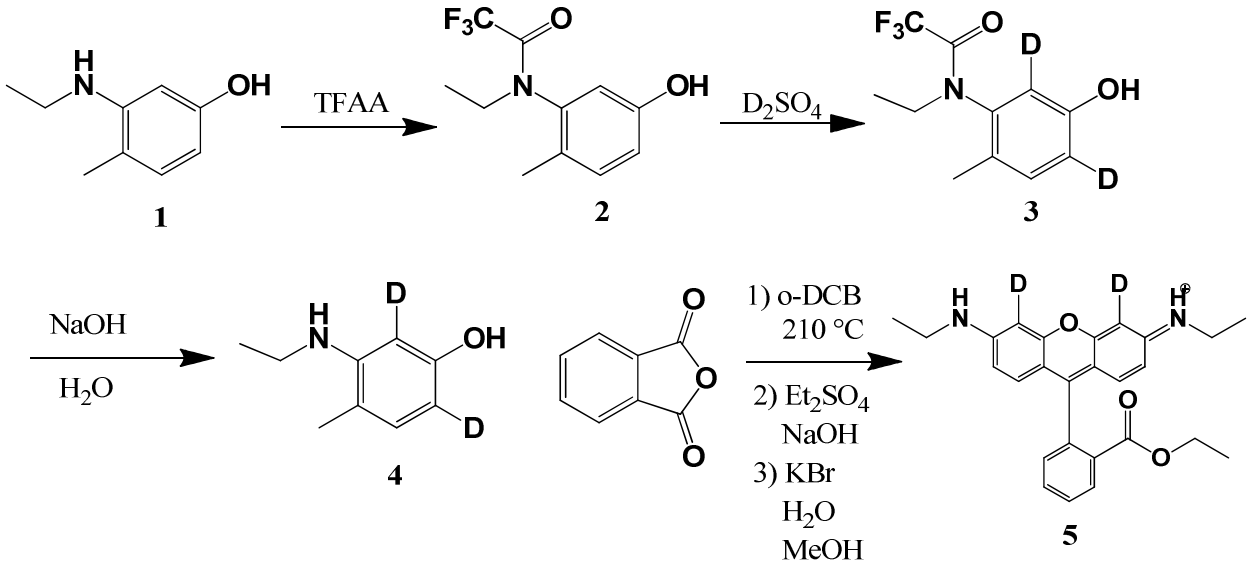

Figure 12: Reaction scheme of R6G-d2.

In order to deuterate the xanthene ring, the deuterium must be on the 3-(ethylamino)-p-cresol (**4**) instead of the pthalic anhydride. Unfortunately, deuterated 3-(ethylamino)-p-cresol is not commercially available and is the synthetic target in order to synthesize R6G-d2. The key to the synthesis of (**4**) is the electrophilic aromatic substitution (EAS) of D^+ which is dictated by the electron density of the ring. The aryl secondary amine and – to a lesser extent – the phenol direct the regioselectivity of the electrophilic substitution. Amines are one of the strongest activating groups for EAS and are ortho/para directors. This is because aryl amines can donate the nitrogen lone pair into the ring system to create the iminium ion to stabilize the intermediate carbocation. Formation of the iminium ion is only possible when the electrophile adds ortho/para to the nitrogen. However, if the aryl amine is protonated, the iminium ion can not be formed, and ring is deactivated. If D_2SO_4 (deuterated sulfuric acid) is added to 3-(ethylamino)-p-cresol (**1**), the aryl amine is protonated which would then promote meta addition; however, the ring was too deactivated and no deuteration occurred (Figure 13). In order to circumvent the protonation of the aryl amine, a protecting group is used. Analogously, acetanilide is known to undergo ortho/para EAS which further confirms that protecting the aryl amine will promote ortho/para directing.[21]

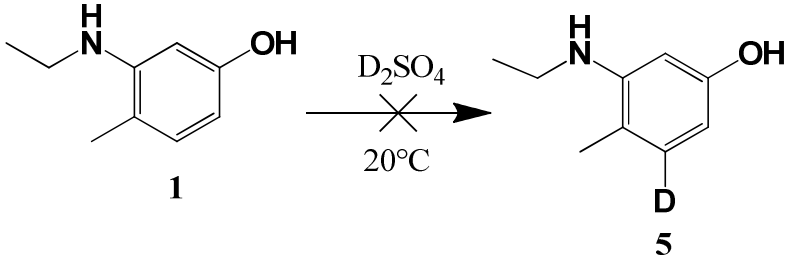

Figure 13: The deuteration of **1** does not occur due to protonation of the aryl amine and deactivation of the ring.

Previous work has suggested that the removal of the trifluoroacetyl protecting group would be challenging. The most successful removal of the group has been with 0.2 M NaOH in water over the course of 72 hours.[22] Other methods were tested to remove the group, including saturated sodium carbonate solution and also p-toluensulfonic acid (p-TsOH)[23] in methanol. The advantage of deprotection of (**3**) using p-TsOH in methanol is that the aqueous work up is bypassed, and water is not introduced. 3-(ethylamino)-p-cresol (**1**) is very polar and has a small pH range where both the phenol is protonated and the amine is not. Bypassing the aqueous extraction would be helpful in improving yields, and more work should be done to implement this technique to the reaction scheme. Unfortunately, R6G-d2 was not synthesized because not enough material of (**4**) could be synthesized.

Synthesis of R6G-d2:

N-ethyl-2,2,2-trifluoro-N-(5-hydroxy-2-methylphenyl)acetamide (2): In a 50 mL round bottom flask, 3-(ethylamino)-p-cresol (**1**) (750 mg, 4.96 mmol) and a magnetic stir bar is added. The round bottom flask is chilled in an ice bath for 10 minutes. Trifluoroacetic anhydride (2 mL, 14.38 mmol) is added slowly with a Pasteur pipette while stirring. The reaction is removed from ice and stirred for 3 hours. The reaction is then purified using flash chromatography on silica gel with a gradient of 10-50% ethyl acetate/hexane. TLC is done using 25% ethyl acetate/hexane. (713.4 mg, 2.89 mmol, 58.1%)

N-Ethyl-2,2,2-trifluoro-N-(4,6-dideutero-5-hydroxy-2-methylphenyl)acetamide (3): In a 50 mL round bottom flask, protected amine (**2**) (293 mg, 1.19 mmol) is stirred at room temperature with 1 mL of CH_2Cl_2 and 1 mL of D_2SO_4 (1.86 g, 18.6 mmol) for 17 hours. Afterwards, the reaction is quenched by pouring into 250 mL round bottom flask with 20 mL of saturate sodium carbonate. The solution is neutralized with HCl to pH 6 and then extracted 2 x 20 mL with CH_2Cl_2. The organic layer is concentrated in vacuo. (59.2 mg, 0.24 mmol, 20%).

2,6-dideutero-3-(ethylamino)-4-methylphenol (4): In a 100 mL round bottom flask, deuterated and protected starting material (**3**) (26 mg, 0.11 mmol) is stirred with 10 mL 50/50% (v/v) water/methanol with sodium carbonate (108 mg, 1.02 mmol) for 72 hours. The solution is then neutralized with 1 M HCl to pH 6 and extracted with 2 x 15 mL CH_2Cl_2. The organic layer is concentrated to yield 13.7 mg (0.091 mmol) of impure product. This product is then deprotected again using 3 mL of 0.2 M NaOH stirred for 17 hours. The solution is neutralized with 1 M HCl then extracted 2 x 10 mL with CH_2Cl_2 and the organic layer is concentrated. (12.8 mg, 0.084 mmol, 76%).

4. Synthesis of Crystal Violet

Crystal violet (CV) became an attractive synthetic target due to its simplistic synthesis, and CV has also been shown to be detected at the single molecule level using SERS.[24] Again the isotopologue method was implemented to statistically support single molecule detection. The isotopologues used for the SM-SERS study was CV-d0 and CV-d12 where the phenyl rings were completely deuterated. In order to maximize the chance of observing spectral shift in hyper Raman, the entire CV molecule was deuterated. CV has a unique synthesis where a Friedel-Crafts alkylation is conducted between carbon tetrachloride and *N,N*-dimethylaniline. Multiple additions of *N,N*-dimethylaniline create the centrosymmetric molecule. The reaction scheme is shown in Figure 14.

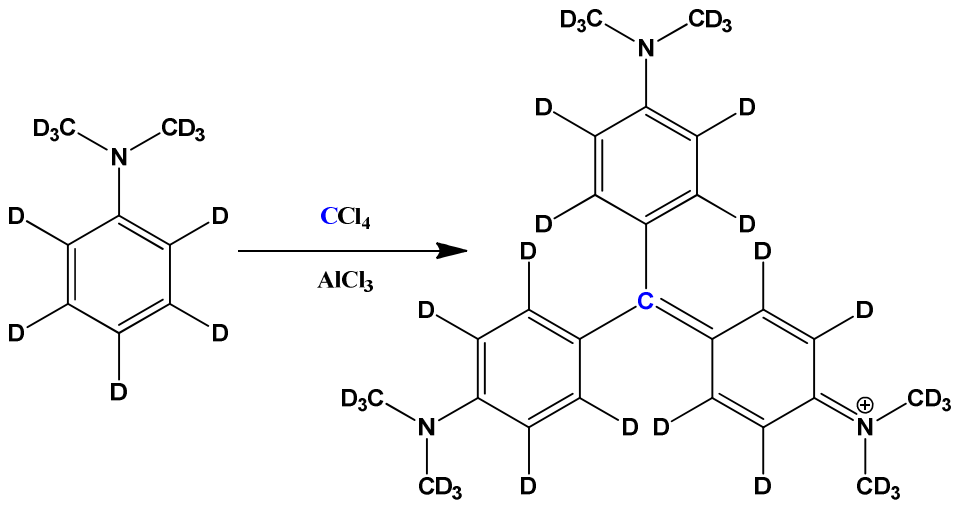

Figure 14: Reaction scheme of CV-d30

The synthesis of CV-d30 proved easier than R6G-d2. However, modifications of the published synthesis were needed. In the synthesis of CV-d12, a dry nitrogen inlet was used to prevent oxygen and water from poisoning the aluminum catalyst. The stream of nitrogen often evaporated the sub-milliliter amount of carbon tetrachloride out of the round bottom flask. An argon balloon was used instead of a nitrogen inlet to prevent evaporation of carbon tetrachloride. After the synthesis of CV-d30, the UV-Vis showed an extra peak that was not found in commercially available CV-d0. The mass spectrum of CV-d30 also had analogous peaks to the CV-d0 under the same instrumental method. This prompted the need to further purify the synthesized compound. By using 5% methanol in CH_2Cl_2, CV had an $R_f = 0.3$ on normal phase silica gel which suggested that a normal phase column could purify the compound. After purification using flash chromatography, the uv-visible absorption (Figure 15) and mass spectrum (Figure 16b) confirmed that CV-d30 was synthesized.

Synthesis of Crystal Violet-d30: The synthesis was modified from Ref. 24.[24] A 25 mL round bottom flask is flamed dried. A magnetic stir bar is added, and the flask is capped with a septum. The flask is then flushed with nitrogen. Fresh anhydrous aluminum trichloride (~100 mg) is removed from a glove box and put into a glass vial for storage. Quickly, aluminum trichloride (22 mg, 0.17 mmol) is removed from the glass vial and added into the round bottom flask. The flask is recapped with a septum and the air removed by vacuum. An argon balloon is then added to the flask. Carbon tetrachloride (250 µL, 2.6 mmol) is added via syringe, and the solution is stirred and heated in an oil bath at 70°C. Once the solution is heated to 70°C, *N,N*-dimethylaniline-d11 (1.0 mL, 8.0 mmol) is added dropwise via syringe to the stirring solution. The solution is then heated and stirred for 15 minutes. Afterwards, the solution is uncapped and quenched by adding the crude to 5g of ice in a 50 mL Erlenmeyer flask. 10 mL of diethyl ether is added to the Erlenmeyer flask, and the solution is extracted 3 x 5 mL with water. CV will be in the aqueous layer. The aqueous layers are combined, and the diethyl ether is discarded. 10 mL of fresh diethyl ether is then added to the aqueous layer, and the aqueous layer is transferred to a clean 50 mL Erlenmeyer flask. To remove the aluminum, sodium bicarbonate (120 mg, 1.43 mmol) is added to the Erlenmeyer flask which is shaken to precipitate $Al(OH)_3$. The aluminum hydroxide is then vacuum filtered using a fritted filter into a 250 mL round bottom flask. The Erlenmeyer is rinsed several times with 10 mL aliquots of water. The filter is then washed 2 x 10 mL of 100% ethanol to ensure all the CV is removed from the filter. The resulting filtered solution is then concentrated to yield CV-d30 (22.3 mg, 0.06 mmol, 2%). A flash chromatography column is then conducted to purify the CV-d30 using a 2% methanol/CH_2Cl_2 to 7% gradient on silica gel. The fractions were collected and concentrated to yield CV-d30.

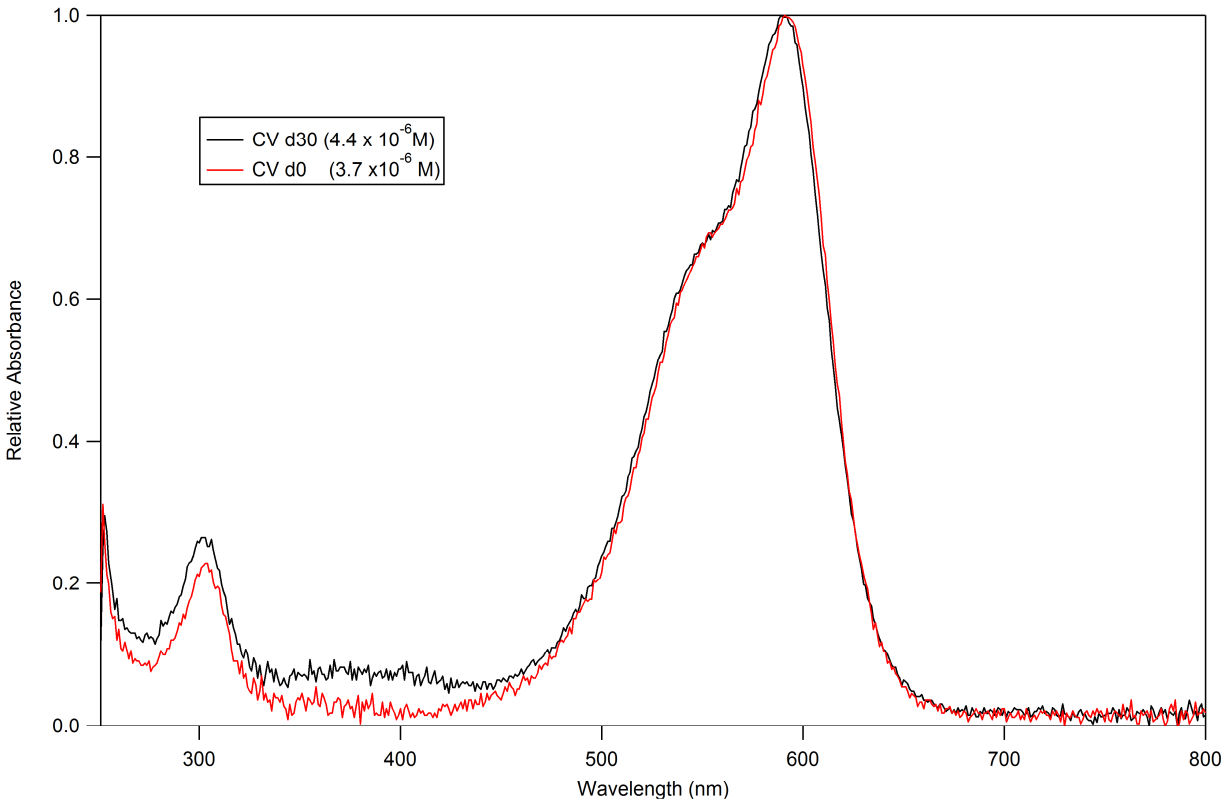

Figure 15: Normalized UV-Vis absorption of synthesized CV-d30 (black) compared to standard CV-d0 (red).

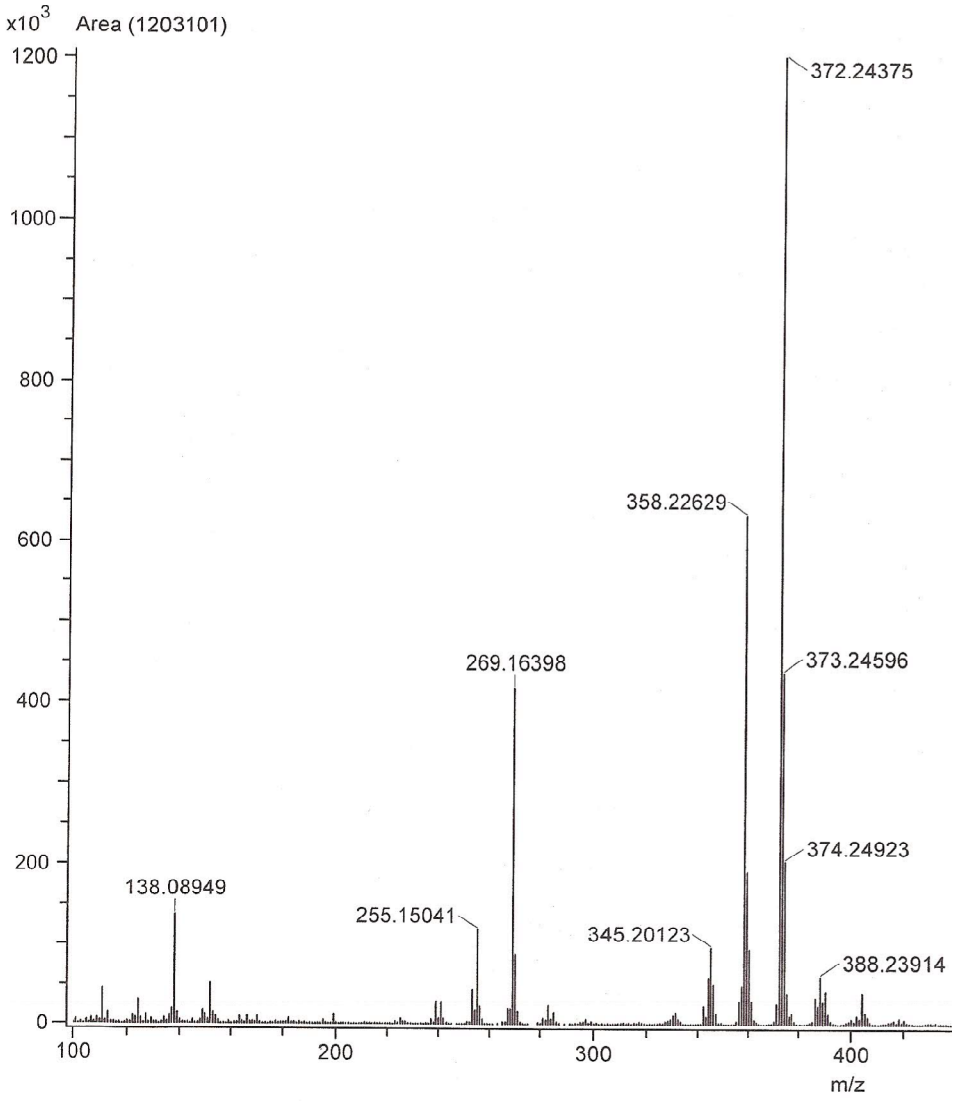

Figure 16a: Mass spectrum of standard CV-d0 using DART-TOF positive ionization. Mass error: 0.5 ppm.

Expected: 372.24 m/z

Measured: 372.24375

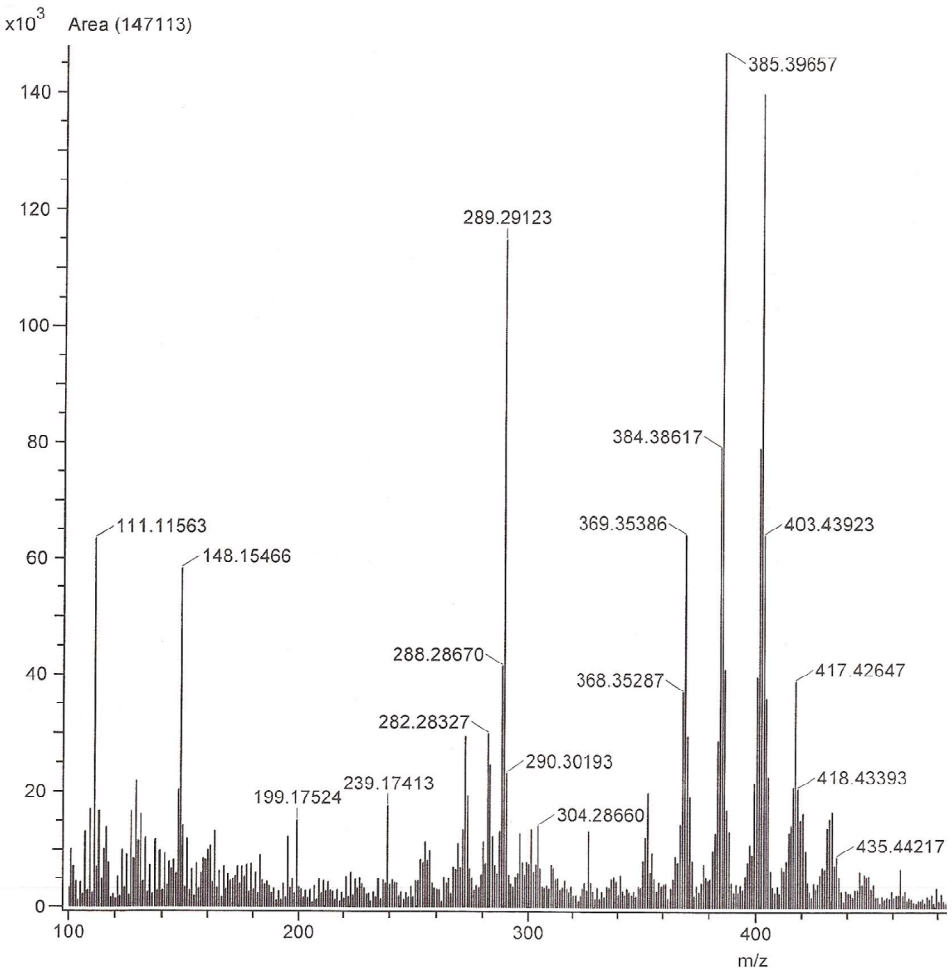

Figure 16b: Mass spectrum of synthesized CV-d30 using DART-TOF positive ionization. Mass error: 1.3 ppm

Expected: 402.43 m/z

Measured: 402.43177

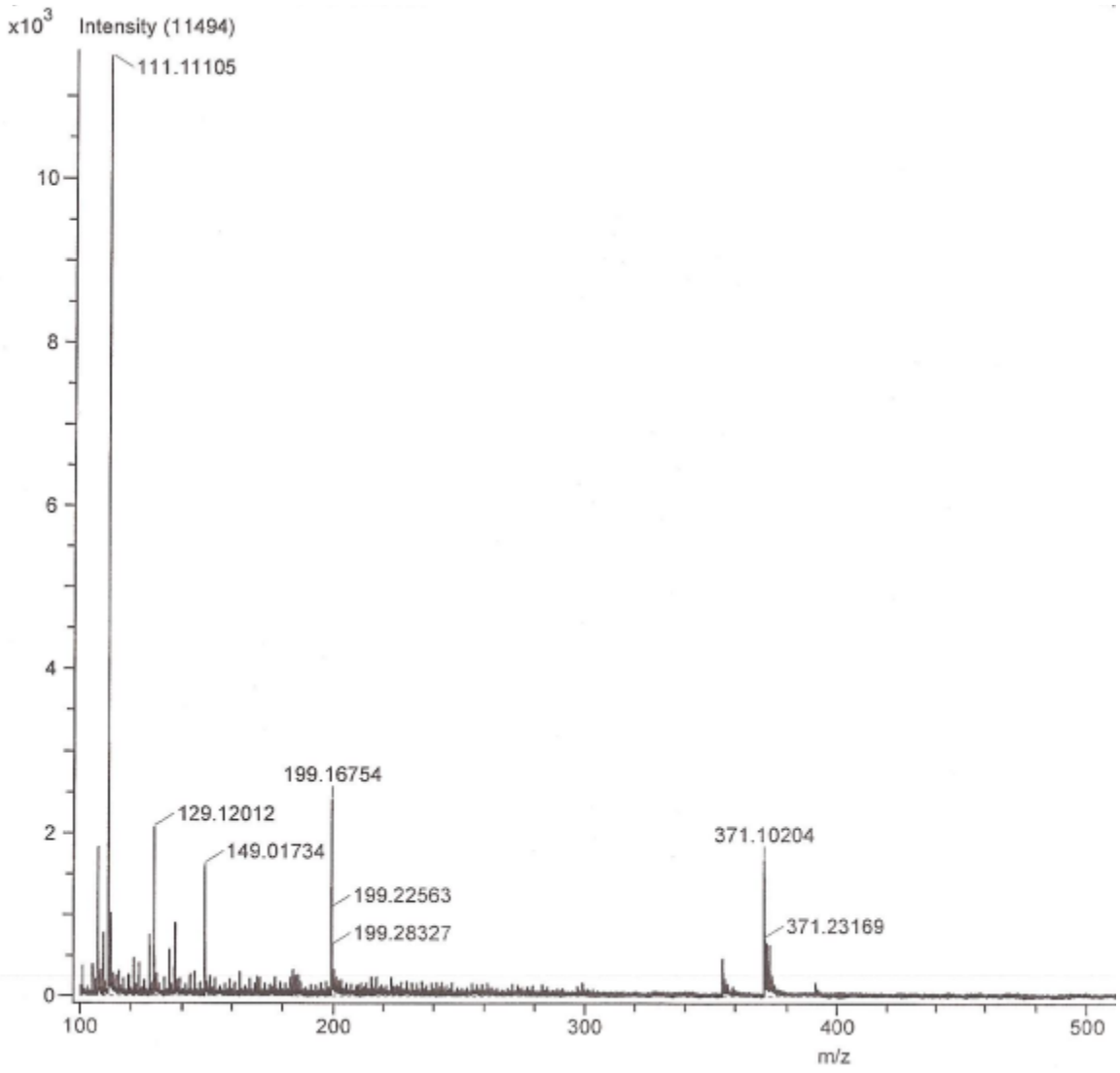

Figure 16c: Background of mass spectrum from DART-TOF positive ionization measured with no sample present.

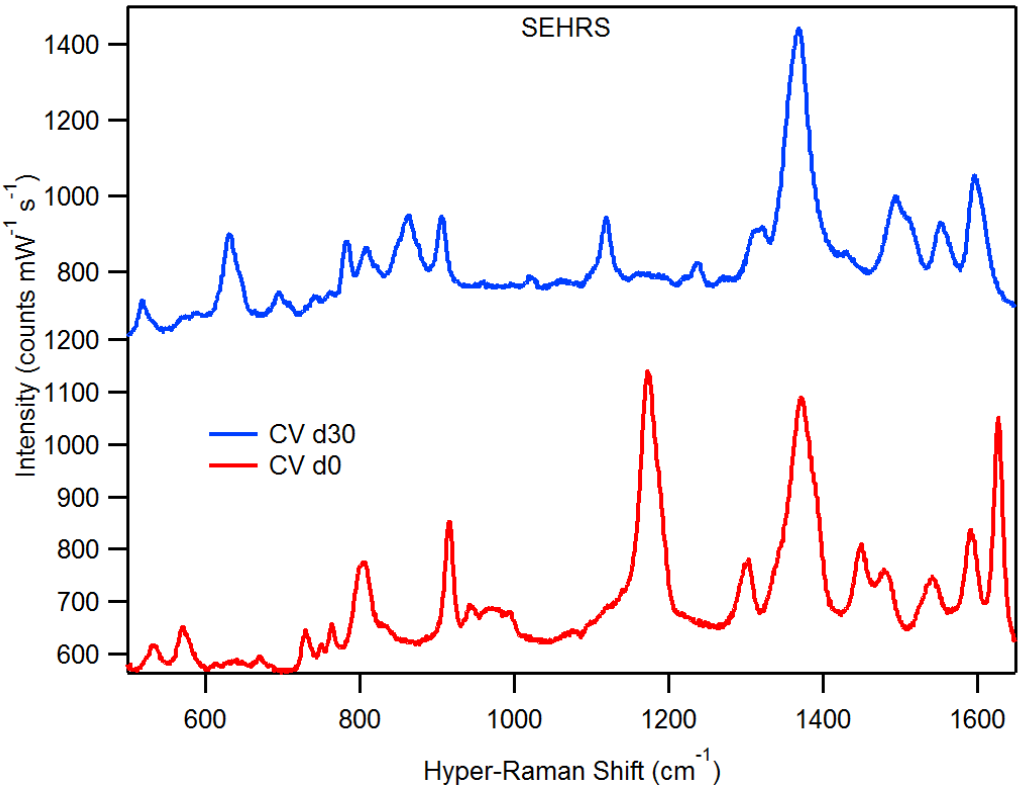

Figure 17: Surface Enhance Hyper Raman of CV-d0 (red) and CV-d30 (blue). The differences in the spectra qualify CV-d30 for SM-SEHRS.

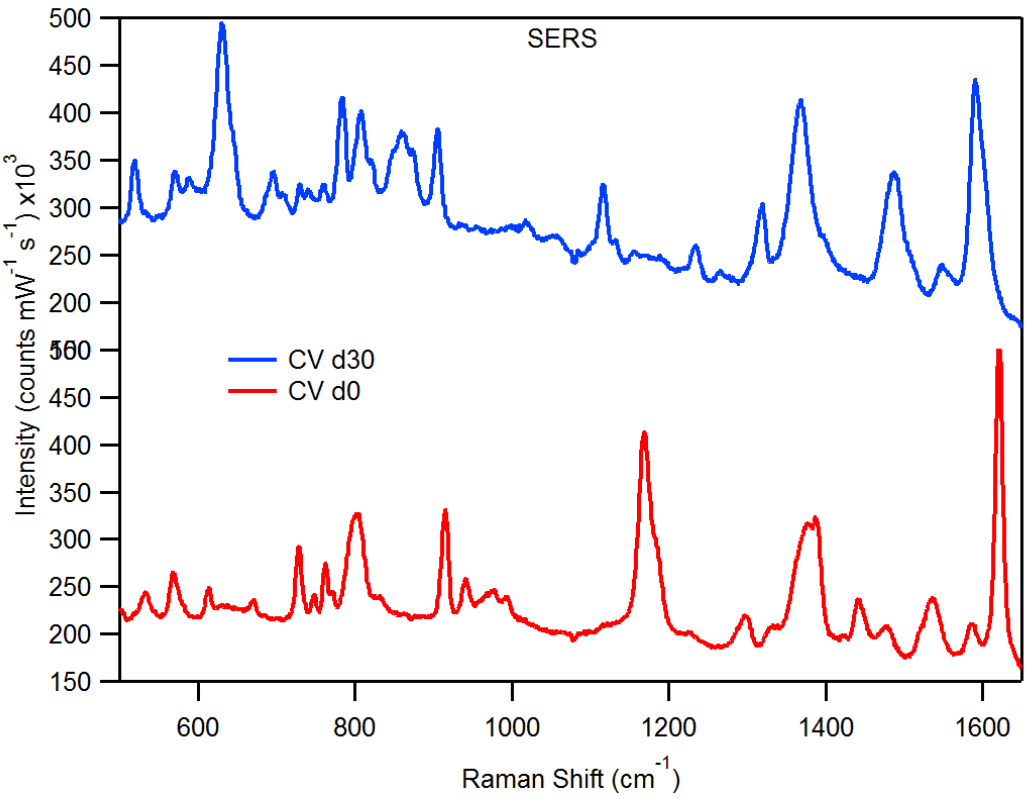

Figure 18: Surface Enhanced Raman Scattering of CV-d0 (red) and CV-d30 (blue).

5. Summary and Outlook

With the successful synthesis of CV-d30, the surface enhanced hyper Raman can be demonstrated at the single molecule level through the isotopologue approach described earlier. Proving that hyper Raman can detect molecules at single molecule sensitivity will help establish hyper Raman as a viable method to study multiphoton processes. Proving single molecule hyper Raman will also be helpful in theoretically modeling the enhancement factors that contribute to the overall hyper Raman process. In addition, isotopologues are helpful for assigning vibrational modes. Features in the vibrational spectra that shift upon deuteration suggest that the isotopes are involved in specific vibrational modes. Future studies could further compare the differences in the SERS and SEHRS of CV isotopologues. Isotopologues of R6G are also of interest because R6G is a model molecule for Raman with thorough theoretical calculations already available for the hyper Raman modes and electronic states. Hopefully, R6G-d2 will be successfully synthesized and the hyper Raman will show a vibrational shift as compared to the R6G-d0. This will confirm speculation that the hyper Raman modes are localized on the xanthene ring.

In conclusion, hyper Raman is an important technique that can probe 1 photon forbidden vibrational transitions as well as exploring 2 photon resonance effects that manifest as vibrational intensity enhancements. The apparent weakness of hyper Raman signal prevents the widespread implementation of hyper Raman to study multiphoton processes. By proving that hyper Raman spectroscopy can probe single molecules is an important result for the widespread adaptation of hyper Raman.

6. NMR

All compounds taken in $CDCl_3$

Compound (**2**)

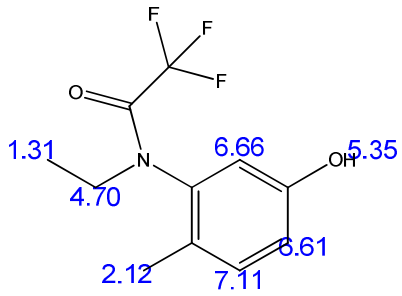

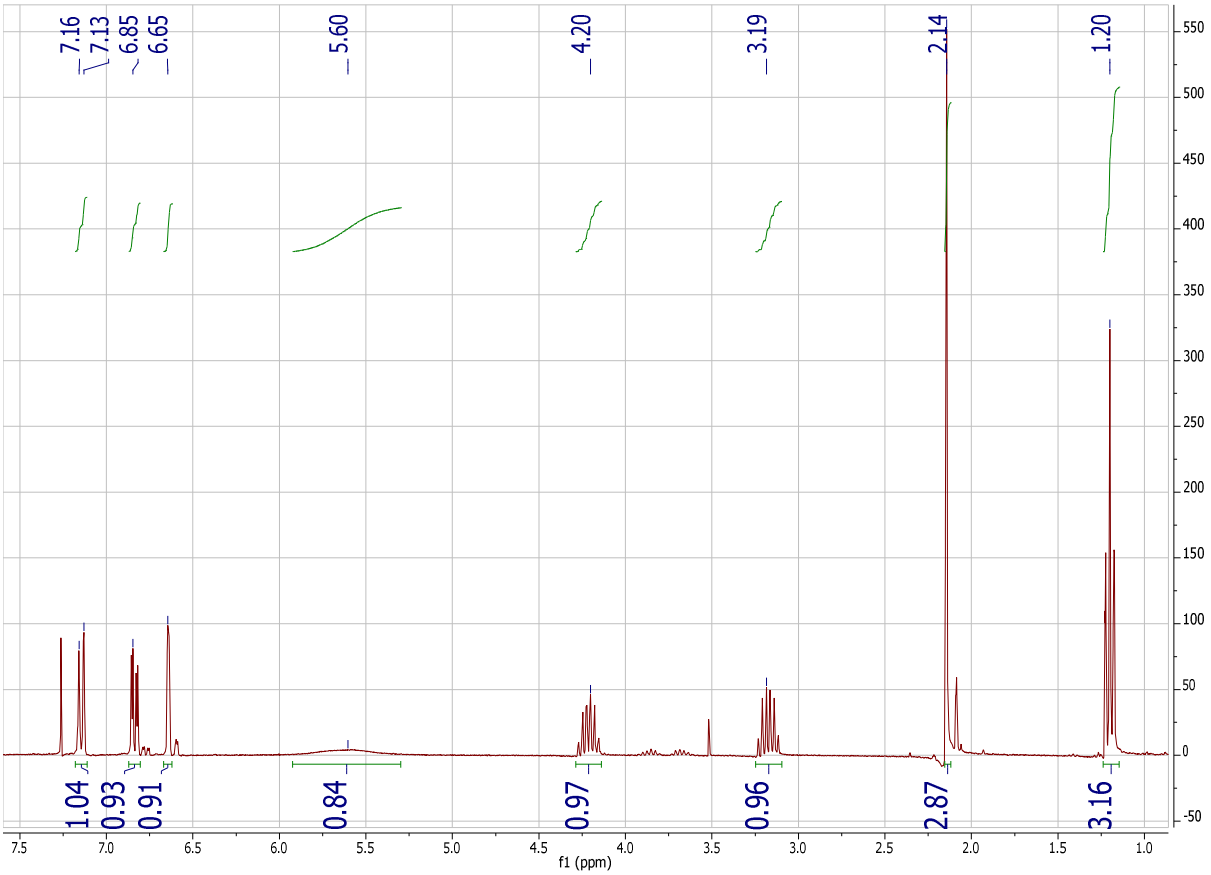

Interestingly, the protons at 4.20 ppm and 3.19 ppm are on the same carbon but are heavily split due to the presence of the trifluoroacetyl protecting group.

Compound (**3**)

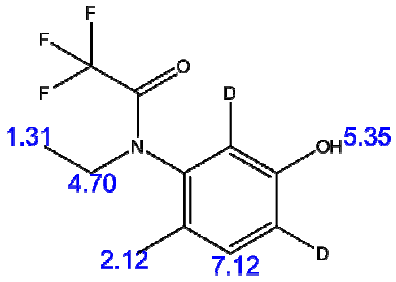

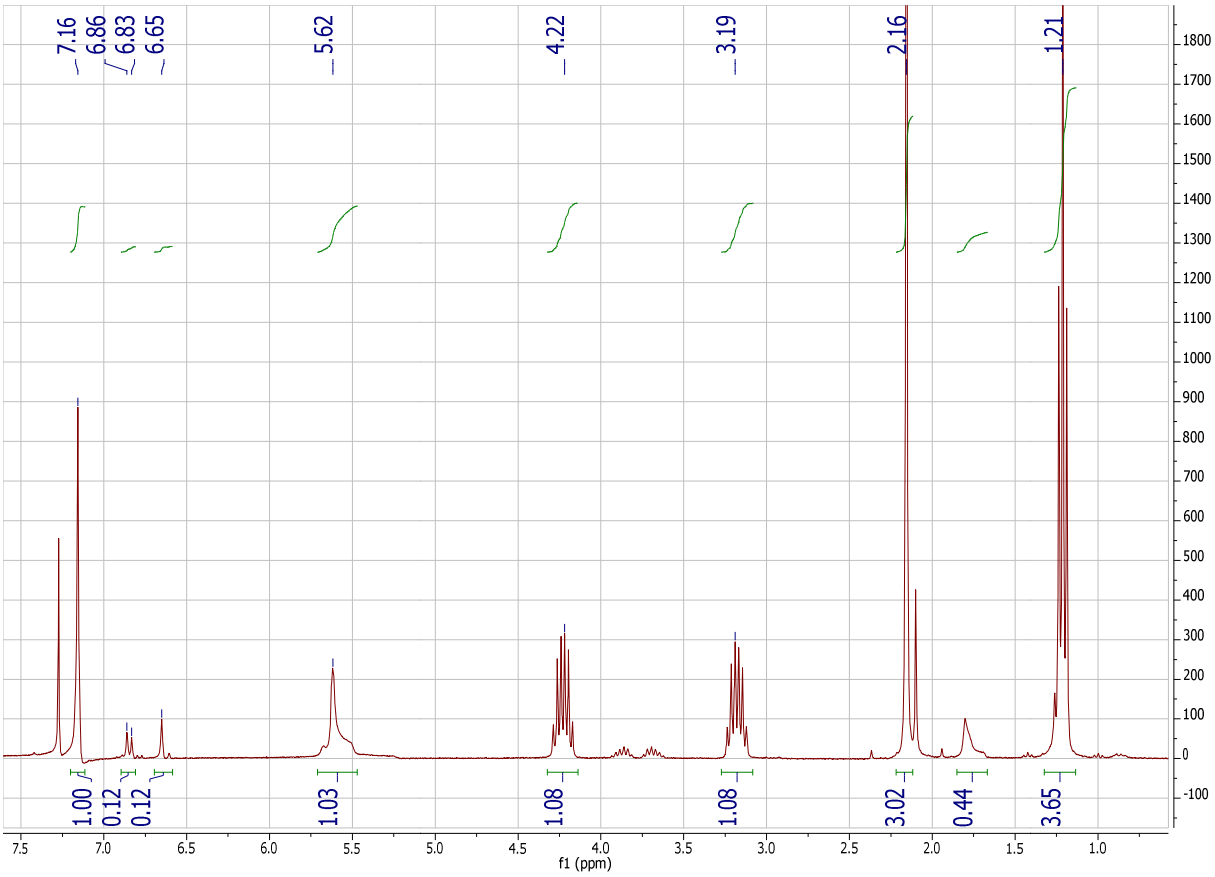

Protons at ethyl carbon still heavily split by protecting group. Deuteration has severely dampened aromatic signal and 7.16 ppm is now a singlet.

Compound (**4**)

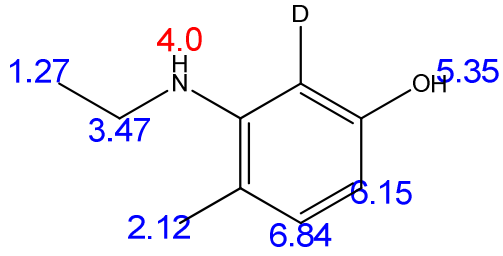

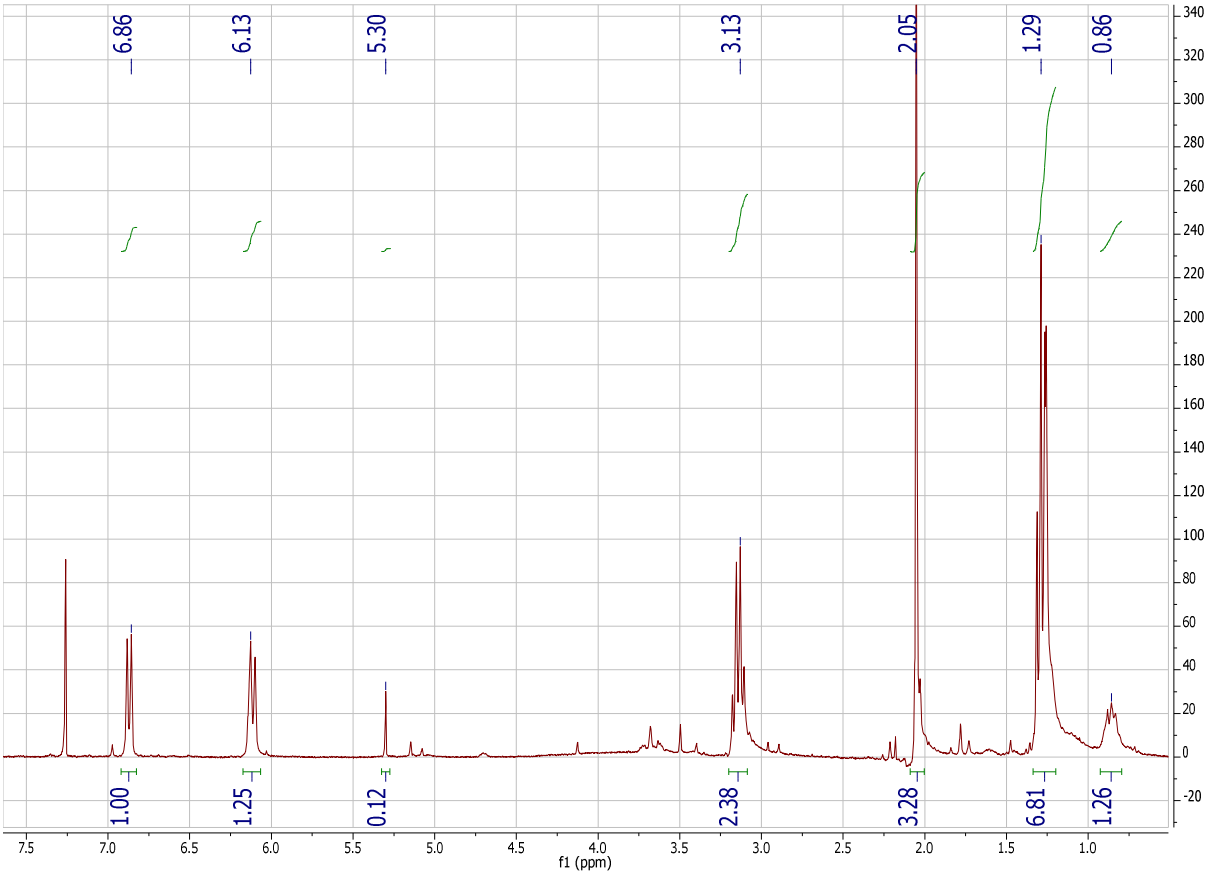

Upon removal of protecting group, ethyl protons no longer split and combine at 3.13 ppm. Proton exchanged during aqueous work up causing doublet of doublets in aromatic region. Deuterium of interest is still ortho to phenol.

7. References

1. McQuarrie, D. A., *Quantum chemistry*. 2nd ed.; University Science Books: Sausalito, Calif., 2008; p xiii, 690 p.
2. Raman, C. V., The Raman effect. Investigation of molecular structure by light scattering. *Trans. Faraday Soc.* **1929,** *25*, 0781-0791.
3. Long, D. A., *The Raman effect : a unified treatment of the theory of Raman scattering by molecules*. Wiley: Chichester ; New York, 2002; p xxiv, 597 p.
4. Milojevich, C. B.; Silverstein, D. W.; Jensen, L.; Camden, J. P., Surface-Enhanced Hyper-Raman Scattering Elucidates the Two-Photon Absorption Spectrum of Rhodamine 6G. *J. Phys. Chem. C* **2013,** *117* (6), 3046-3054.
5. Moerner, W. E.; Fromm, D. P., Methods of single-molecule fluorescence spectroscopy and microscopy. *Rev. Sci. Instrum.* **2003,** *74* (8), 3597-3619.
6. Orrit, M.; Bernard, J., SINGLE PENTACENE MOLECULES DETECTED BY FLUORESCENCE EXCITATION IN A PARA-TERPHENYL CRYSTAL. *Phys. Rev. Lett.* **1990,** *65* (21), 2716-2719.
7. Andersen, P. C.; Jacobson, M. L.; Rowlen, K. L., Flashy silver nanoparticles. *J. Phys. Chem. B* **2004,** *108* (7), 2148-2153.
8. Domke, K. F.; Zhang, D.; Pettinger, B., Enhanced Raman spectroscopy: Single molecules or carbon? *J. Phys. Chem. C* **2007,** *111* (24), 8611-8616.
9. Le Ru, E. C.; Blackie, E.; Meyer, M.; Etchegoin, P. G., Surface enhanced Raman scattering enhancement factors: a comprehensive study. *J. Phys. Chem. C* **2007,** *111* (37), 13794-13803.
10. Dieringer, J. A.; Lettan, R. B.; Scheidt, K. A.; Van Duyne, R. P., A frequency domain existence proof of single-molecule surface-enhanced Raman Spectroscopy. *J. Am. Chem. Soc.* **2007,** *129* (51), 16249-16256.
11. Hovel, H.; Fritz, S.; Hilger, A.; Kreibig, U.; Vollmer, M., WIDTH OF CLUSTER PLASMON RESONANCES - BULK DIELECTRIC FUNCTIONS AND CHEMICAL INTERFACE DAMPING. *Phys. Rev. B* **1993,** *48* (24), 18178-18188.
12. Lee, P. C.; Meisel, D., ADSORPTION AND SURFACE-ENHANCED RAMAN OF DYES ON SILVER AND GOLD SOLS. *J. Phys. Chem.* **1982,** *86* (17), 3391-3395.
13. Hao, E.; Schatz, G. C., Electromagnetic fields around silver nanoparticles and dimers. *J. Chem. Phys.* **2004,** *120* (1), 357-366.
14. Lu, X. M.; Rycenga, M.; Skrabalak, S. E.; Wiley, B.; Xia, Y. N., Chemical Synthesis of Novel Plasmonic Nanoparticles. In *Annual Review of Physical Chemistry*, Annual Reviews: Palo Alto, 2009; Vol. 60, pp 167-192.
15. Im, S. H.; Lee, Y. T.; Wiley, B.; Xia, Y. N., Large-scale synthesis of silver nanocubes: The role of HCl in promoting cube perfection and monodispersity. *Angew. Chem.-Int. Edit.* **2005,** *44* (14), 2154-2157.
16. Wiley, B. J.; Xiong, Y. J.; Li, Z. Y.; Yin, Y. D.; Xia, Y. N., Right bipyramids of silver: A new shape derived from single twinned seeds. *Nano Lett.* **2006,** *6* (4), 765-768.
17. Grabar, K. C.; Freeman, R. G.; Hommer, M. B.; Natan, M. J., PREPARATION AND CHARACTERIZATION OF AU COLLOID MONOLAYERS. *Anal. Chem.* **1995,** *67* (4), 735-743.

18. Jin, R. C.; Cao, Y. W.; Mirkin, C. A.; Kelly, K. L.; Schatz, G. C.; Zheng, J. G., Photoinduced conversion of silver nanospheres to nanoprisms. *Science* **2001,** *294* (5548), 1901-1903.
19. Xue, C.; Metraux, G. S.; Millstone, J. E.; Mirkin, C. A., Mechanistic study of photomediated triangular silver nanoprism growth. *J. Am. Chem. Soc.* **2008,** *130* (26), 8337-8344.
20. Jin, R. C.; Cao, Y. C.; Hao, E. C.; Metraux, G. S.; Schatz, G. C.; Mirkin, C. A., Controlling anisotropic nanoparticle growth through plasmon excitation. *Nature* **2003,** *425* (6957), 487-490.
21. Sanchez-Viesca, F.; Gomez, M. R. G.; Berros, M., Electric Hindrance and Precursor Complexes in the Regiochemistry of Some Nitrations. *J. Chem. Educ.* **2011,** *88* (7), 944-946.
22. Isidro-Llobet, A.; Alvarez, M.; Albericio, F., Amino Acid-Protecting Groups. *Chem. Rev.* **2009,** *109* (6), 2455-2504.
23. Spencer, C.; Balsells, J.; Li, H. M., Practical cleavage of trifluoroacetamides with p-toluensulfonic acid. *Tetrahedron Lett.* **2009,** *50* (9), 1010-1012.
24. Kleinman, S. L.; Ringe, E.; Valley, N.; Wustholz, K. L.; Phillips, E.; Scheidt, K. A.; Schatz, G. C.; Van Duyne, R. P., Single-Molecule Surface-Enhanced Raman Spectroscopy of Crystal Violet Isotopologues: Theory and Experiment. *J. Am. Chem. Soc.* **2011,** *133* (11), 4115-4122.